ADVANCED MATERIALS
www.advmat.de

Digitalizing Self-Assembled Chiral Superstructures for Optical Vortex Processing

Peng Chen, Ling-Ling Ma, Wei Duan, Ji Chen, Shi-Jun Ge, Zhi-Han Zhu, Ming-Jie Tang, Ran Xu, Wei Gao, Tao Li, Wei Hu, and Yan-Qing Lu**

Cholesteric liquid crystal (CLC) chiral superstructures exhibit unique features; that is, polychromatic and spin-determined phase modulation. Here, a concept for digitalized chiral superstructures is proposed, which further enables the arbitrary manipulation of reflective geometric phase and may significantly upgrade existing optical apparatus. By encoding a specifically designed binary pattern, an innovative CLC optical vortex (OV) processor is demonstrated. Up to 25 different OVs are extracted with equal efficiency over a wavelength range of 116 nm. The multiplexed OVs can be detected simultaneously without mode crosstalk or distortion, permitting a polychromatic, large-capacity, and in situ method for parallel OV processing. Such complex but easily fabricated self-assembled chiral superstructures exhibit versatile functionalities, and provide a satisfactory platform for OV manipulation and other cutting-edge territories. This work is a vital step towards extending the fundamental understanding and fantastic applications of ordered soft matter.

Chiral superstructures are ubiquitous wonders found in galaxies, bindweed plants, beetle exoskeletons,[1] DNA, and so on. They trigger curiosities toward insights of intriguing natural materials and inspire novel artificial architectures.[2] Thanks to the intrinsic rapid and cost-effective formation, self-assembled soft matter is a promising candidate for building up such chiral superstructures. Among them, cholesteric liquid crystal (CLC) is a fascinating building block with wide feature size range and extra-field tunability.[3,4] Such chiral liquid crystal (LC) has long been a booming topic in material science and is actively being pursued in numerous application fields, including reflective displays,[5] switchable polarizers and color filters,[6] nonmechanical beam steering,[7,8] and mirrorless tunable lasers.[9]

CLC is a liquid crystalline phase where the rod-like molecules self-assemble into a periodic helical structure, and forms a natural 1D soft photonic crystal. These chiral superstructures exhibit a broadband Bragg reflection with unique circular-polarization (spin) selectivity.[10] Very recently, the spin–orbit geometric phase was discovered for the light reflected off planar CLC chiral superstructures, and immediately attracts extensive attention.[11–13] It supplies a new platform for broadband reflective geometric phase manipulation.[14] Meanwhile, the transmitted light just experiences a uniform dynamic phase change. That enables a spin-determined phase modulation. Above features introduced by CLC superstructures may significantly upgrade existing optical apparatuses. In case that such helical nanoarchitectures could be rationally encoded in a point-to-point manner, photonic devices with advanced functionalities based on fantastic chiral superstructures will be reasonably expected. Unfortunately, freely designing and arbitrarily tailoring chiral superstructures remain highly restricted, which is an urgent task to be addressed.

In this work, we propose a digitalized chiral superstructure, where both initial and terminal orientations of CLC standing helixes are binarily encoded in plane. The self-assembly of such 3D CLC superstructures is guided by two parallel preprogrammed photoalignment films. Through imprinting a Dammann vortex grating (DVG)[15] pattern into a planar CLC, an optical vortex (OV, Supporting Information 1)[16] processor is demonstrated. Polychromatic OVs carrying multiplexed orbital angular momentum (OAM)[17] are simultaneously detected in a nondestructive way. This offers a practical and robust approach for in situ and parallel OV processing in OAM incorporated wavelength-division multiplexing (WDM), which is expecting to dramatically expand the communication capacity.[18] This work provides an open-ended strategy for designing and tailoring chiral superstructures, and may promote applications in versatile fields.

For the light propagating along the CLC helix axis, a circular-polarization selective Bragg reflection is exhibited over a wavelength range $n_o p$–$n_e p$, where p is the helical pitch, and n_o/n_e are the ordinary/extraordinary refractive indices, respectively.[19] The circularly polarized light with the same handedness as the

P. Chen, L.-L. Ma, W. Duan, J. Chen, S.-J. Ge, M.-J. Tang, R. Xu, Prof. T. Li, Prof. W. Hu, Prof. Y.-Q. Lu
National Laboratory of Solid State Microstructures
College of Engineering and Applied Sciences
and Collaborative Innovation Center of Advanced Microstructures
Nanjing University
Nanjing 210093, China
E-mail: huwei@nju.edu.cn; yqlu@nju.edu.cn
Dr. Z.-H. Zhu, Prof. W. Gao
Da-Heng Collaborative Innovation Center for Science of Quantum Manipulation and Control
Harbin University of Science and Technology
Harbin 150080, China
The ORCID identification number(s) for the author(s) of this article can be found under https://doi.org/10.1002/adma.201705865.

DOI: 10.1002/adma.201705865

 © 2018 WILEY-VCH Verlag GmbH & Co. KGaA, Weinheim

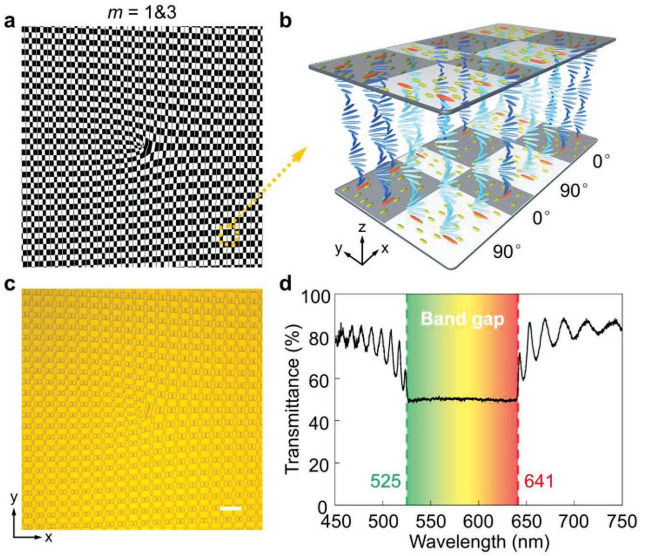

Figure 1. Schematics and characterizations of the digitalized CLC superstructures. a) The phase pattern of a 2 × 5 DVG with $m_x = 1$ and $m_y = 3$, where black indicates 0 and white indicates π. b) A right-handed CLC superstructure encoded with the DVG corresponding to the region marked in dash line in (a), with z along the axis of the helical structure. The director adjacent to the substrate is marked in red and photoalignment agent molecules in yellow. CLC helixes with orthogonal planar alignment are represented by cyan and blue. c) The image of the CLC DVG recorded under reflective mode of an optical microscope; the scale bar is 100 µm. d) The transmission spectra of the CLCs for linearly polarized (LP) light. The Bragg photonic band gap is indicated with corresponding colors.

chiral helix of CLCs is reflected, while the opposite polarized one is transmitted. For inhomogeneous CLC superstructures, the reflective geometric phase change is twice the initial/terminal orientation angle of local standing helix, and exhibits a handedness-dependent sign.[11,13]

Referring to above rules, via properly digitalizing the chiral superstructures, binary optics based on reflective geometric phase can be freely designed and realized. Moreover, it possesses unique properties of nondestruction and broadband equal-high efficiency. For instance, a DVG pattern composed of certain binary phase (0 and π) regions[20] is introduced to digitalize CLCs. **Figure 1**a shows the phase pattern of a 2 × 5 DVG with $m_x = 1$ and $m_y = 3$ (m_x/m_y is the topological charge of the DVG in x/y dimension). Accordingly, the helix axes of digitalized CLC superstructures stand normally to the substrate while the director orientations (α, with respect to the x axis) at both substrates follow

$$\alpha = \frac{\varphi_{\mathrm{DVG}}(x,y)}{2} \tag{1}$$

where $\varphi_{\mathrm{DVG}}(x,y)$ is the phase function of a DVG. Figure 1b schematically depicts a right-handed CLC superstructure encoded with the DVG, where the initial (terminal) orientations of CLC helixes are 0° and 90° alternatively.

When a plane wave whose wavelength falls within the Bragg photonic band gap ($n_o p$–$n_e p$) is normally incident, the right circular polarization (RCP) component will be reflectively diffracted into desired OV orders carrying different topological charges (m). OV possesses a helical phase profile of $e^{im\phi}$ and an OAM of $m\hbar$ per photon.[17] In case of an OV incident, certain diffraction order(s) will turn to a central bright spot, which can serve as the criteria for OV detection (see Supporting Information text 2 for detailed analysis). The left circular polarization (LCP) is transmitted without spatial phase difference, making a spin-determined semitransparent device possible. Besides, the spatial separation of multiple OAM states can greatly extend the detection range of m, avoiding mode overlap and facilitating high-capacity parallel processing.

Compared to conventional contact techniques for LC alignment, photoalignment is a promising approach for high-quality and high-resolution multidomain LC alignment avoiding any mechanical damage, electrostatic charge, or dust contamination.[21] These years have witnessed a rapid development of LC photoalignment, especially in information display industry. Here, a polarization-sensitive sulfonic azo dye SD1 (Figure S1, Supporting Information) was used as the photoalignment agent, whose molecules tend to reorient their absorption oscillators perpendicular to the polarization direction of the illuminating UV light and further guide LCs.[22] To digitalize CLC chiral superstructures, a two-step photoexposure process was performed through the dynamic photopatterning technology.[23] At first, the cell is uniformly exposed with linearly polarized UV light, and then is exposed again to receive the DVG pattern with the polarizer rotating 90°. The exposed areas are realigned to be orthogonal to the first orientation. Therefore, the two substrates are synchronously imprinted with alternative 0° and 90° alignment consistent with the DVG pattern.

We adopted a large-birefringence nematic LC NJU-LDn-4[24] doped with a right-handed chiral dopant R5011. As shown in Figure 1d, a Bragg reflection is exhibited between 525 and 641 nm ($\Delta\lambda$ = 116 nm) covering green to red. After infiltrated into the photopatterned cell, both initial and terminal orientations of CLC standing helixes are controlled by adjacent SD1 molecules on substrates. The binarily encoded local orientations (0° and 90°) make the neighbored CLCs self-assemble into two different kinds of helixes (90° rotation with each other). Thus, the designed chiral superstructure is realized as shown in Figure 1b. The image in Figure 1c is consistent with the DVG pattern in Figure 1a. All regions are uniform in brightness and color, which matches the center wavelength of the Bragg band in Figure 1d. Thanks to the specific phase modulation of CLC, the RCP light will be reflected and imprinted a binary phase profile (0 and π) of the desired DVG pattern, while the LCP will be transmitted and remain the original phase-front.

The optical setup for OV processing based on digitalized CLC superstructures is illustrated in **Figure 2**a. To explore the polychromatic behavior of the CLC DVG, different lasers (λ = 532, 580, 600, and 633 nm) are utilized. The OV generation capability is first demonstrated (Figure 2b–e). As expected, 2 × 5 donut-like reflected diffraction orders (n_x, n_y) carrying topological charge $m = n_x + 3n_y$ (corresponding to OAM range of −5 – +5) are clearly observed. The phase singularity results in a donut-like intensity profile, whose radius increases with $|m|$. The sign of m reflects the handedness of the OVs helical phase. The diffraction efficiencies (η) of all ten OVs are measured for different λ, where η is defined as the intensity ratio of objective

© 2018 WILEY-VCH Verlag GmbH & Co. KGaA, Weinheim

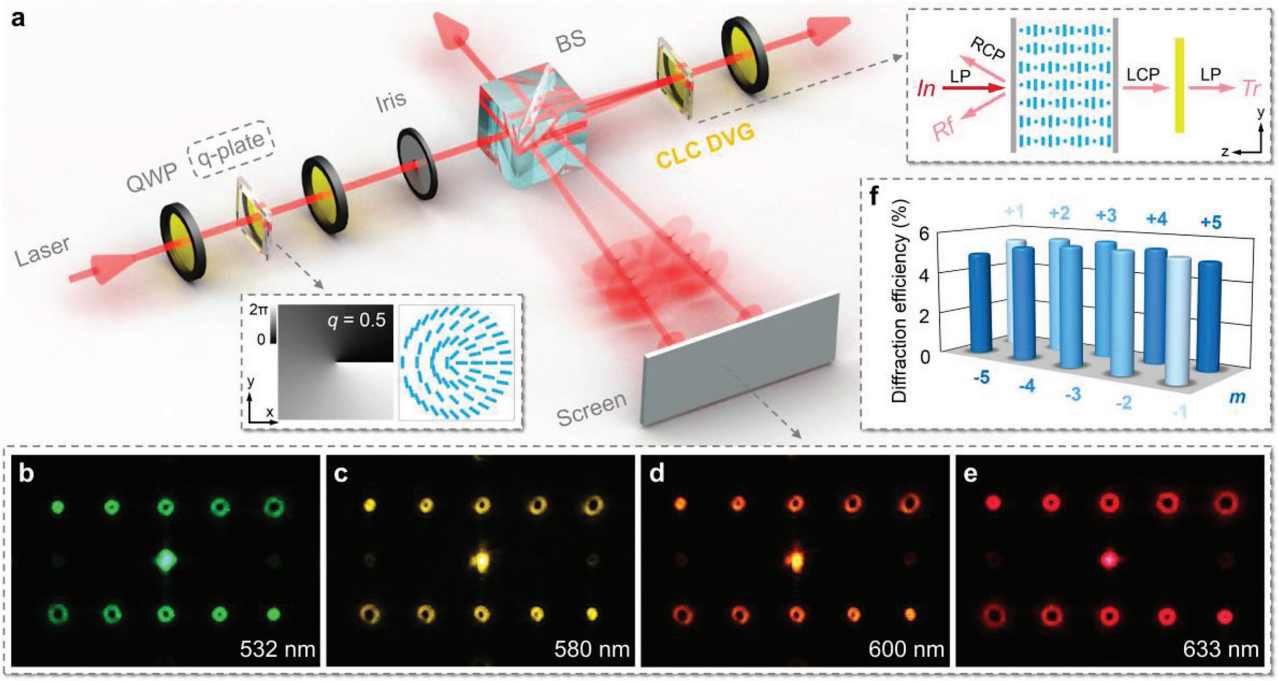

Figure 2. Polychromatic OV generation from digitalized CLC superstructures. a) The optical setup for OV processing. QWP, quarter-wave plate; BS, nonpolarizing beam splitter. Insets: the theoretical phase pattern and corresponding director distribution of an LC q-plate with $q = 0.5$; the side-view schematic of the director distribution of the CLC DVG with the polarization states of the incident (In), reflected (Rf), and transmitted (Tr) light labeled, respectively. The reflected diffraction patterns at different wavelengths of b) 532 nm, c) 580 nm, d) 600 nm, and e) 633 nm. f) The average diffraction efficiency of all ten OVs with $m = -5 - +5$ for measured wavelengths, where the errors are all less than 0.2%.

diffraction order to the total reflected light. Figure 2f shows the average η with respective m labeled, which is almost equal (≈5.4%). The total reflected diffraction efficiency is $\eta = 54.3\% \pm 0.3\%$, approaching the theoretical value of 62.7%.[20] Above results verify that a large range of OAM states can be extracted in broad band, good energy uniformity, and high efficiency.

In addition to OV generation, the digitalized CLC superstructures can also be employed for OV detection. Here, the OVs to be detected are generated by a nematic LC q-plate,[25] a type of transmissive geometric phase element (see Supporting Information text 3). In Figure 2a, the sandwiched q-plate between quarter-wave plates (QWPs) are used to generate linearly polarized OV. The image of a q-plate with $q = 0.5$ is exhibited in **Figure 3**b, where a gradual change of the brightness can be observed due to the continuous varying of the director as depicted in the inset in Figure 2a. In our experiments, a voltage

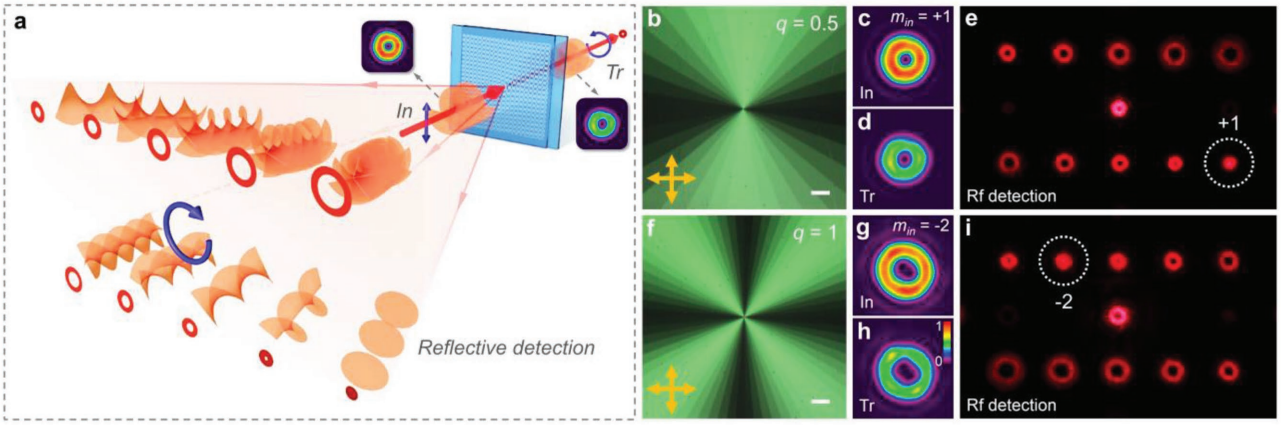

Figure 3. Single OAM detection by digitalized CLC superstructures. a) Schematic illustration for the detection. The polarization states of the incident, reflected, and transmitted light are indicated with blue arrows. Insets: intensity images of incident and transmitted OV. b,f) Images of q-plates with $q = 0.5$ and $q = 1$, respectively. The polarizer and analyzer are indicated by double-ended arrows, and scale bars are 100 µm. c,g) the incident, d,h) transmitted OVs, and e,i) reflective diffraction patterns with $m_{in} = +1$ and $m_{in} = -2$, respectively. The color bars indicate the relative optical intensity. The detected OAM modes are marked in dashed circles.

© 2018 WILEY-VCH Verlag GmbH & Co. KGaA, Weinheim

of 2.5 V is applied to the *q*-plate to keep the half-wave condition at 633 nm. The resultant OV with $m_{in} = +1$ (Figure 3c) illuminates the CLC DVG as schematically illustrated in Figure 3a. The reflected diffraction pattern and transmitted light are shown in Figure 3e,d, respectively. Compared to Figure 2e, all diffraction orders turn to $n_x + 3n_y + 1$ and the order (+2, −1) is recovered to a Gaussian beam with a central bright spot, verifying $m_{in} = +1$. The transmitted light (Figure 3d) remains the same as the incident (Figure 3c) except for an overall intensity decreasing. Besides, the detection results for $m_{in} = -2$ are also shown in Figure 3g–i.

The simultaneous detection of mixed OAM states is crucial in OAM-based optical communications and quantum optics. Here, we propose a multi-*q*-plate to directly generate multi-OAM states (see Supporting Information text 4 for details). The theoretical phase patterns, images and director distributions of four different examples are shown in **Figure 4**. For multi-OAM with opposite signs and same values, the phase/director distributions are binary and thus, corresponding images (Figure 4a,d; Figure S2, Supporting Information) hold uniform brightness and color. While for multi-OAM with different values, the continuous brightness change consists with corresponding phase pattern, and several spatially separated singular points are observed (Figure 4b,c). The detection results for these multiplexed OAMs containing large m_{in} and up to four OAM states are demonstrated subsequently. The central bright spots of specific diffraction orders reveal OAM components of the incident OVs. Through this method, different OAMs are transformed to separate partial-Gaussian beams and then can be efficiently coupled into respective channels in demultiplexing process. Particularly, the semitransparent feature enables the digitalized CLC superstructure to serve as an in situ OAM demultiplexer. Moreover, the results at 532 nm are demonstrated as well in Figure S3 of the Supporting Information.

Traditional transmissive LC elements suffer from intense wavelength-dependent efficiency.[26] By contrast, the CLC DVG here is polychromatic and perfectly tolerant with existing WDM technologies. Furthermore, the helical pitch and even the handedness of CLCs are sensitive to electric field[11] and light irradiation.[4,7] Although only results in visible band are presented, by properly changing the concentration of chiral dopant, external field applied or the angle of incident beam,[14] the wavelength range can be rationally controlled to cover the commonly used communication bands. Additionally, the device can be tuned from fully reflective to totally transmissive via altering the incident polarization owing to the spin-dependent reflection of CLC chiral superstructures. Over 97% intensity of the transmitted mode is preserved except for a little diffraction loss. The intensity of 0th order in the reflected pattern is slightly stronger, attributed to the Fresnel reflection. Fortunately, this issue

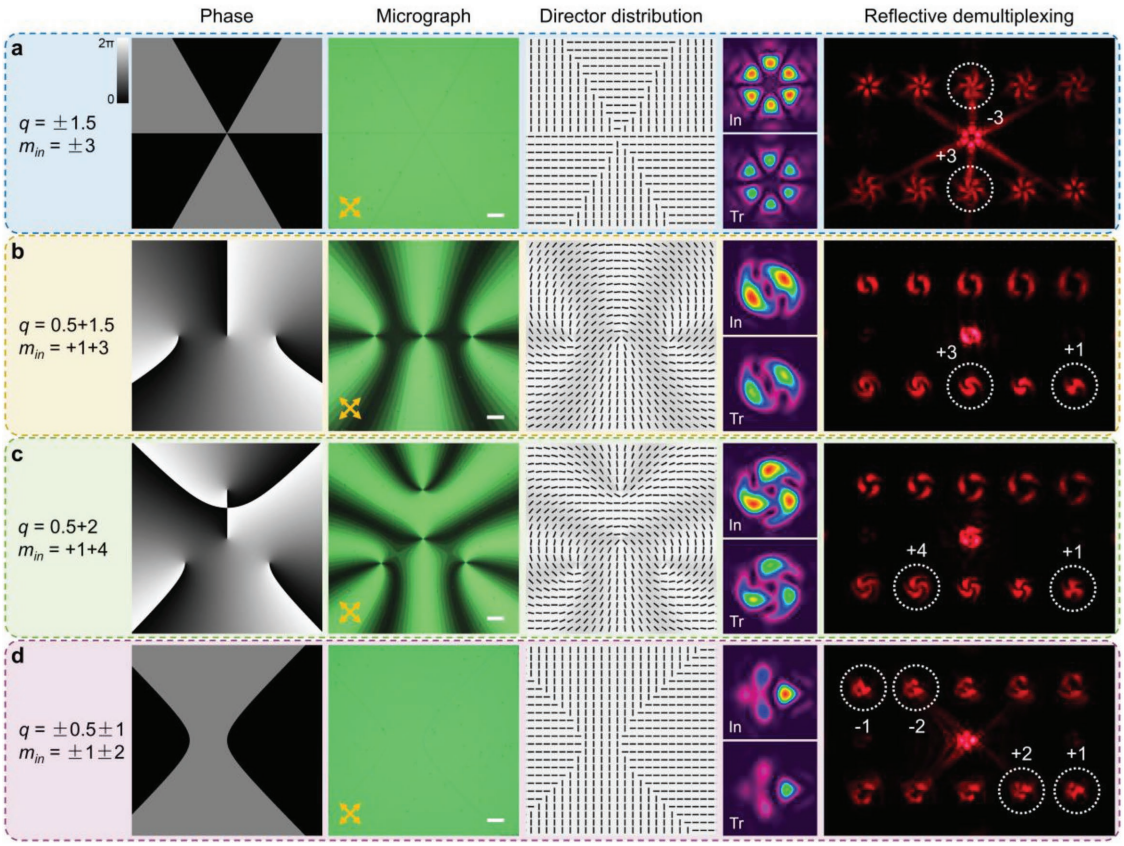

Figure 4. Multiplexed OAM demultiplexing via digitalized CLC superstructures. The phase patterns, images, and director distributions of the multi-*q*-plates with a) $q = \pm 1.5$, b) $q = 0.5 + 1.5$, c) $q = 0.5 + 2$, and d) $q = \pm 0.5 \pm 1$, respectively. The color variation from black to white indicates the phase varying from 0 to 2π. All scale bars are 100 µm. The intensity images of the incident, transmitted light and reflective demultiplexing of (a) $m_{in} = \pm 3$, (b) $m_{in} = +1 + 3$, (c) $m_{in} = +1 + 4$, and (d) $m_{in} = \pm 1 \pm 2$, respectively.

© 2018 WILEY-VCH Verlag GmbH & Co. KGaA, Weinheim

could be satisfactorily addressed by antireflection coating. The OV processing range can be further extended by appropriately designing Dammann structures. Figure S4 of the Supporting Information exhibits a 5 × 5 CLC DVG, whose polychromatic OV processing range is from −12 to +12. Thanks to the intrinsic self-organization of CLCs, such DVGs are easy-fabrication and cost efficient compared to artificial chiral nanostructures.[27] The collaboration of the "top-down" photopatterning process and "bottom-up" self-assembly pushes the tailoring of chiral superstructures into an unprecedented level. The concept proposed in this work is not restricted to DVG pattern, further digitalizing CLCs with other distinctive patterns may open up more fruitful functionalities.

In conclusion, a concept of digitalized chiral superstructures is proposed and demonstrated via photoaligning CLCs. Besides unique features of polychromatic and spin-determined phase modulation, our work further makes the flexible manipulation of reflective geometric phase available. On the basis of a DVG encoded CLC superstructure, the generation, detection, and demultiplexing of OVs are presented. It offers a robust and innovative strategy for OV processing in a polychromatic, large-capacity, and in situ way, lightening the OAM-based optical communications. Such complex but easy-fabrication chiral superstructures exhibit fancy and versatile functionalities, and may directly satisfy tough requirements in some cutting-edge territories. In all, it is an important step forward to extending the fundamental understanding and fantastic applications of ordered soft matters.

Experimental Section

Sample Fabrication: Indium-tin-oxide glass substrates (1.5 × 2 cm^2) were ultrasonically bathed, UV-ozone cleaned, and then spin-coated with the photoalignment agent SD1 (Dai-Nippon Ink and Chemicals, Japan, whose chemical structure is shown in Figure S1, Supporting Information), which was dissolved in dimethylformamide at a concentration of 0.3 wt%. After curing at 100 °C for 10 min, two pieces of glass substrates were assembled and sealed with epoxy glue to form a cell with a gap of 6 µm. For CLC DVGs, the empty cell was placed at the image plane of the DMD-based microlithography system to accomplish a uniform alignment and then record the DVG patterns with the orthogonal exposure polarization. For nematic LC (multi-)*q*-plates, a multistep partly overlapping exposure process[28] was performed to carry out the designed director distributions accordingly.

LC Materials: The utilized CLC was prepared by mixing a home-made nematic LC NJU-LDn-4 (Δn = 0.353, and extraordinary refractive index n_e = 1.867 at 589 nm and 20 °C, clearing point T_c = 157 °C)[24] with 3.1 wt% right-handed chiral dopant R5011 (HCCH, China). The CLC was infiltrated into the DVG-patterned cell at 160 °C and gradually cooled to room temperature. The nematic LC E7 was purchased from HCCH (Δn = 0.223 at 589 nm and 20 °C, T_c = 59.7 °C). The E7 was infiltrated into the (multi-)*q*-plate-patterned cell at 70 °C and cooled to room temperature.

Characterizations: The images of CLC DVGs were recorded under the reflective mode of an optical microscope (Nikon 50i, Japan), while those of (multi-)*q*-plates under the transmissive mode with crossed polarizer and analyzer. The wavelength range of the white-light supercontinuum laser (WL-SC-400, Fianium, UK) is 400–2400 nm, and filtered for different monochromatic wavelengths by the acousto-optic tunable filter. Reflected diffraction patterns from CLC DVGs were captured by a digital camera (EOS M, Canon, Japan). The incident and transmitted OVs were captured by a CCD camera (BGS-SP620, Ophir-Spiricon, USA).

Supporting Information

Supporting Information is available from the Wiley Online Library or from the author.

Acknowledgements

This work was supported by the National Key Research and Development Program of China (2017YFA0303700), the National Natural Science Foundation of China (NSFC) (Nos. 61490714, 61435008, 61575093, and 11574065), and the Fundamental Research Funds for the Central Universities and the Special funds for Excellence Science Team of HUST (No. 289991703).

Conflict of Interest

The authors declare no conflict of interest.

Keywords

chiral superstructures, cholesteric liquid crystals, photoalignment

Received: October 9, 2017
Revised: December 12, 2017
Published online: January 15, 2018

[1] V. Sharma, M. Crne, J. O. Park, M. Srinivasarao, *Science* **2009**, *325*, 449.
[2] A. Kuzyk, R. Schreiber, Z. Fan, G. Pardatscher, E. M. Roller, A. Högele, F. C. Simmel, A. O. Govorov, T. Liedl, *Nature* **2012**, *483*, 311.
[3] R. Eelkema, M. M. Pollard, N. Katsonis, J. Vicario, D. J. Broer, B. L. Feringa, *J. Am. Chem. Soc.* **2006**, *128*, 14397.
[4] H. K. Bisoyi, Q. Li, *Chem. Rev.* **2016**, *116*, 15089.
[5] S. T. Wu, D. K. Yang, *Reflective Liquid Crystal Displays*, Wiley, New York, NY **2001**.
[6] Y. Wang, Q. Li, *Adv. Mater.* **2012**, *24*, 1926.
[7] Z. G. Zheng, Y. Li, H. K. Bisoyi, L. Wang, T. J. Bunning, Q. Li, *Nature* **2016**, *531*, 352.
[8] C. C. Li, C. W. Chen, C. K. Yu, H. C. Jau, J. A. Lv, X. Qing, C. F. Lin, C. Y. Cheng, C. Y. Wang, J. Wei, Y. L. Yu, T. H. Lin, *Adv. Opt. Mater.* **2017**, *5*, 1600824.
[9] a) H. Coles, S. Morris, *Nat. Photonics* **2010**, *4*, 676; b) J. Xiang, A. Varanytsia, F. Minkowski, D. A. Paterson, J. M. Storey, C. T. Imrie, O. D. Lavrentovich, P. Palffy-Muhoray, *Proc. Natl. Acad. Sci. USA* **2016**, *113*, 12925.
[10] I. C. Khoo, S. T. Wu, *Optics and Nonlinear Optics of Liquid Crystals*, World Scientific, Singapore **1993**.
[11] J. Kobashi, H. Yoshida, M. Ozaki, *Nat. Photonics* **2016**, *10*, 389.
[12] M. Rafayelyan, G. Tkachenko, E. Brasselet, *Phys. Rev. Lett.* **2016**, *116*, 253902.
[13] R. Barboza, U. Bortolozzo, M. G. Clerc, S. Residori, *Phys. Rev. Lett.* **2016**, *117*, 053903.
[14] a) J. Kobashi, H. Yoshida, M. Ozaki, *Phys. Rev. Lett.* **2016**, *116*, 253903; b) M. Rafayelyan, E. Brasselet, *Opt. Lett.* **2016**, *41*, 3972.
[15] T. Lei, M. Zhang, Y. R. Li, P. Jia, G. N. Liu, X. G. Xu, Z. H. Li, C. J. Min, J. Lin, C. Y. Yu, H. B. Niu, X. C. Yuan, *Light Sci. Appl.* **2015**, *4*, e257.

 © 2018 WILEY-VCH Verlag GmbH & Co. KGaA, Weinheim

[16] a) S. Franke-Arnold, L. Allen, M. Padgett, *Laser Photonics Rev.* **2008**, *2*, 299; b) M. Q. Mehmood, S. Mei, S. Hussain, K. Huang, S. Y. Siew, L. Zhang, T. Zhang, X. Ling, H. Liu, J. Teng, A. Danner, S. Zhang, C. W. Qiu, *Adv. Mater.* **2016**, *28*, 2533.
[17] L. Allen, M. W. Beijersbergen, R. Spreeuw, J. Woerdman, *Phys. Rev. A* **1992**, *45*, 8185.
[18] a) J. Wang, J. Y. Yang, I. M. Fazal, N. Ahmed, Y. Yan, H. Huang, Y. X. Ren, Y. Yue, S. Dolinar, M. Tur, A. E. Willner, *Nat. Photonics* **2012**, *6*, 488; b) A. E. Willner, H. Huang, Y. Yan, Y. Ren, N. Ahmed, G. Xie, C. Bao, L. Li, Y. Cao, Z. Zhao, J. Wang, M. P. J. Lavery, M. Tur, S. Ramachandran, A. F. Molisch, N. Ashrafi, S. Ashrafi, *Adv. Opt. Photonics* **2015**, *7*, 66.
[19] P. Yeh, C. Gu, *Optics of Liquid Crystal Displays*, Wiley, New York, NY **1999**.
[20] C. Zhou, L. Liu, *Appl. Opt.* **1995**, *34*, 5961.
[21] a) M. Schadt, H. Seiberle, A. Schuster, *Nature* **1996**, *381*, 212; b) T. Du, J. Schneider, A. K. Srivastava, A. S. Susha, V. G. Chigrinov, H. S. Kwok, A. L. Rogach, *ACS Nano* **2015**, *9*, 11049; c) Y. Guo, M. Jiang, C. Peng, K. Sun, O. Yaroshchuk, O. Lavrentovich, Q. H. Wei, *Adv. Mater.* **2016**, *28*, 2353.
[22] V. Chigrinov, S. Pikin, A. Verevochnikov, V. Kozenkov, M. Khazimullin, J. Ho, D. D. Huang, H. S. Kwok, *Phys. Rev. E* **2004**, *69*, 061713.
[23] L. L. Ma, M. J. Tang, W. Hu, Z. Q. Cui, S. J. Ge, P. Chen, L. J. Chen, H. Qian, L. F. Chi, Y. Q. Lu, *Adv. Mater.* **2017**, *29*, 1606671.
[24] L. Wang, X. W. Lin, X. Liang, J. B. Wu, W. Hu, Z. G. Zheng, B. B. Jin, Y. Q. Qin, Y. Q. Lu, *Opt. Mater. Express* **2012**, *2*, 1314.
[25] L. Marrucci, C. Manzo, D. Paparo, *Phys. Rev. Lett.* **2006**, *96*, 163905.
[26] J. Kim, Y. Li, M. N. Miskiewicz, C. Oh, M. W. Kudenov, M. J. Escuti, *Optica* **2015**, *2*, 958.
[27] J. K. Gansel, M. Thiel, M. S. Rill, M. Decker, K. Bade, V. Saile, G. von Freymann, S. Linden, M. Wegener, *Science* **2009**, *325*, 1513.
[28] P. Chen, S. J. Ge, W. Duan, B. Y. Wei, G. X. Cui, W. Hu, Y. Q. Lu, *ACS Photonics* **2017**, *4*, 1333.

© 2018 WILEY-VCH Verlag GmbH & Co. KGaA, Weinheim